Inorg. Chem. **2002**, *41*, 1306–1314

Ligand Substitution Kinetics of the Iron(III) Hydroxo Dimer with Simple Inorganic Ligands

Gábor Lente and István Fábián*

University of Debrecen, Department of Inorganic and Analytical Chemistry, Debrecen 10, P.O.B. 21, Hungary, H-4010

Received September 27, 2001

The kinetics and mechanisms of ligand substitution reactions of the iron(III) hydroxo dimer, $Fe_2(\mu\text{-}OH)_2(H_2O)_8^{4+}$, with various inorganic ligands were studied by the stopped-flow method at 10.0 or 25.0 °C in 1.0 M $NaClO_4$. The transient formation of the following di- and tetranuclear complexes was confirmed: $Fe_2(OH)SO_4^{3+}$, $Fe_2(OH)H_2PO_2^{4+}$, $Fe_2(OH)HPO_3^{3+}$, $Fe_2(OH)SeO_3^{3+}$, and $Fe_4(AsO_4)(OH)_2^{7+}$. The catalytic effect of arsenic(III) on the hydrolytic reaction of iron(III) was also attributed to the formation of a dinuclear complex at very low concentration levels. Fast formation and subsequent dissociation of the multinuclear species into the corresponding mononuclear complexes (FeL) proceed via parallel reaction paths which, in general, show composite pH dependencies. The appropriate rate laws were established. The reactions of the different ligands occur at very similar rates, though the uninegatively charged singly deprotonated form reacts about 1 order of magnitude faster than the neutral form of the same ligand. The results can conveniently be interpreted in terms of a dissociative interchange mechanism which postulates the formation of an intermediate complex in which the ligand is coordinated to only one Fe(III) center of the hydroxo dimer. In a subsequent fast step, the ligand forms a bridge between the two metal ions by replacing one of the OH groups. The dissociation of the dinuclear complex into FeL most likely proceeds via the same intermediate.

Introduction

Aqueous iron(III) is known to form hydrolytic complexes[1] even at relatively low pH, where the dominant forms are $FeOH^{2+}$, $Fe(OH)_2^{+}$, and $Fe_2(OH)_2^{4+}$.[2−7] The equilibria between monomeric species are likely to be diffusion-controlled,[8] while the formation and dissociation of the hydroxo dimer can be studied conveniently by the stopped-flow method.[6,9] Our studies with sulfite[10] and phosphate[11] ions confirmed the formation of transient multinuclear complexes with $Fe_2(OH)_2^{4+}$. Similar complexes were also reported with a few organic ligands.[12−14]

In this work, we report our results on the reactions of $Fe_2(OH)_2^{4+}$ with sulfate, selenite, hypophosphite, phosphite, and arsenate ions.[15] A test method[16] showed that two additional simple inorganic ions, dithionite and periodate ions, also react directly with $Fe_2(OH)_2^{4+}$. However, these reactions show complex kinetic patterns which cannot be interpreted in terms of simple ligand substitution reactions and were excluded from the present study.

We also describe an unexpected kinetic phenomenon in the arsenite ion−iron(III) system. Although arsenite ion forms no detectable complex with iron(III) in the pH range studied (pH < 2.20), it catalyzes the formation and dissociation of the $Fe_2(OH)_2^{4+}$ complex.

Experimental Section

Reagents. Low chloride iron(III) perchlorate (Aldrich) was used without further purification. The iron(III) and free acid concentrations of the iron(III) stock solutions were determined as described

* Author to whom correspondence should be addressed. E-mail: ifabian@delfin.klte.hu.

(1) We assume that the iron(III) complexes are octahedral, and the coordinated water molecules are not given in the formulas.

(2) Knight, R. J.; Sylva, R. N. *J. Inorg. Nucl. Chem.* **1974**, *36*, 591.
(3) Ciavatta, L.; Grimaldi, M. *J. Inorg. Nucl. Chem.* **1975**, *37*, 163.
(4) Flynn, C. M. *Chem. Rev.* **1984**, *84*, 31.
(5) Khoe, G. H.; Brown, P. L.; Sylva, R. N.; Robbins, R. G. *J. Chem. Soc., Dalton Trans.* **1986**, 1901.
(6) Lente, G.; Fábián, I. *Inorg. Chem.* **1999**, *38*, 603.
(7) Byrne, R. H.; Luo, Y. R.; Young, R. W. *Mar. Chem.* **2000**, *70*, 23.
(8) Hemmes, P.; Rich, L. D.; Cole, D. L.; Eyring, E. M. *J. Phys. Chem.* **1971**, *75*, 929.
(9) Sommer, B. A.; Margerum, D. W. *Inorg. Chem.* **1970**, *9*, 2517.
(10) Lente, G.; Fábián, I. *Inorg. Chem.* **1998**, *37*, 4204.
(11) Lente, G.; Magalhães, M. E. A.; Fábián, I. *Inorg. Chem.* **2000**, *39*, 1950.
(12) Sisley, M. J.; Jordan, R. B. *Inorg. Chem.* **1991**, *30*, 2190.
(13) Chatlas, J.; Jordan, R. B. *Inorg. Chem.* **1994**, *33*, 3817.
(14) Sisley, M. J.; Jordan, R. B. *Inorg. Chem.* **1995**, *34*, 6015.
(15) The terms sulfate ion, phosphite ion, and so forth are used in a general sense throughout the text and stand for all protonated forms of the ligands, which are only distinguished when it is required for the clarity of the presentation.
(16) Lente, G.; Fábián, I. *React. Kinet. Catal. Lett.* **2001**, *73*, 117.

10.1021/ic011013w CCC: $22.00
Published on Web 02/14/2002

earlier.[17,18] No aging effects were observed in the iron(III) stock solutions during the entire study. All solutions were prepared with doubly deionized and ultrafiltered water obtained from a MILLI-Q RG (Millipore) water purification system. Experiments were carried out at 10.0 ± 0.1 or 25.0 ± 0.1 °C; the ionic strength was set to 1.0 M with high purity $NaClO_4$ (Fluka).

Sodium arsenite stock solutions were prepared by dissolving a weighed quantity of primary standard As_2O_3 (Reanal, Hungary) in NaOH followed by neutralization with $HClO_4$.[19] Stock solutions of other ligands were prepared using analytical reagent grade $Na_2HAsO_4 \cdot 7H_2O$, $Na_2SO_4 \cdot 10H_2O$, $Na_2HPO_3 \cdot 5H_2O$, H_3PO_3, H_2SeO_3, and $NaH_2PO_2 \cdot H_2O$. Stock solutions of arsenate, phosphite, and selenite ions were standardized by acid−base titrations.

Instrumentation and Computation. An Applied Photophysics DX-17 MV sequential stopped-flow apparatus (dead time:[20] 1.1 ± 0.1 ms) was used for kinetic studies with 10 and 2 mm optical path lengths. The pH (=−log[H^+]), which never exceeded 2.20, was calculated from the composition of the samples using the corresponding stability constants. UV−vis spectra were recorded on a HP-8543 diode-array or a Unicam Helios α scanning spectrophotometer. A GK2401C combination electrode was used for pH measurements with a PHM85 pH meter (Radiometer), and the pH meter readings were converted into [H^+] as described earlier.[21] The software packages PSEQUAD[22] and SCIENTIST[23] were used for nonlinear least-squares fitting. Kinetic model calculations were carried out as reported in our previous studies.[11,24−26]

Results

Protolytic Equilibria. The following equilibria are important in dilute, acidic solutions of iron(III):[2−14]

$$Fe^{3+} \rightleftharpoons FeOH^{2+} + H^+ \quad \beta_1 = \frac{[FeOH^{2+}][H^+]}{[Fe^{3+}]} \tag{1}$$

$$Fe^{3+} \rightleftharpoons Fe(OH)_2{}^+ + 2H^+ \quad \beta_2 = \frac{[Fe(OH)_2{}^+][H^+]^2}{[Fe^{3+}]} \tag{2}$$

$$2Fe^{3+} \rightleftharpoons Fe_2(OH)_2{}^{4+} + 2H^+ \quad \beta_3 = \frac{[Fe_2(OH)_2{}^{4+}][H^+]^2}{[Fe^{3+}]^2} \tag{3}$$

Equilibrium constants used in this study are summarized in Table 1. Polynuclear or colloidal hydroxo species[4,7] are not formed under the conditions applied here.

Reactions 1 and 2 can be treated as fast equilibria on the stopped-flow time scale,[8] while the dissociation of $Fe_2(OH)_2{}^{4+}$ is relatively slow with a lifetime of 1−10 s at room temperature:[6,9]

$$Fe_2(OH)_2{}^{4+} \rightleftharpoons 2FeOH^{2+} \tag{4}$$

Recently, it was shown that any shift in the hydrolytic equilibria of iron(III) results in a first-order kinetic process,

Table 1. Equilibrium Constants of Protolytic and Complex Formation Reactions, μ = 1.0 M ($NaClO_4$)

reaction	log K	T (°C)	method[a]	ref
$Fe^{3+} = FeOH^{2+} + H^+$ (β_1)	−3.03	10.0	UV−vis	10
	−2.72	25.0	UV−vis	6
$2Fe^{3+} = Fe_2(OH)_2{}^{4+} + 2H^+$ (β_3)	−2.98	10.0	UV−vis	10
	−2.86	25.0	UV−vis	6
$Fe^{3+} = Fe(OH)_2{}^+ + 2H^+$ (β_2)	−6.7	10.0	est	11
	−6.29	25.0	pH	5
$H_2AsO_4^- + H^+ = H_3AsO_4$	2.05 ± 0.02	10.0	pH	*b*
	2.25[c]	18	pH	27
$HAsO_4^{2-} + H^+ = H_2AsO_4^-$	6.19 ± 0.02	10.0	pH	*b*
	6.77[c]	18	pH	27
$HSeO_3^- + H^+ = H_2SeO_3$	2.59 ± 0.02	10.0	UV−vis	*b*
	2.27	25	pH	28
$SeO_3^{2-} + H^+ = HSeO_3^-$	7.55 ± 0.05	10.0	UV−vis	*b*
	7.78	25	pH	28
$H_2PO_2^- + H^+ = H_3PO_2$	0.87 ± 0.03	10.0	cplx	*b*
	0.87[d]	25.0	pH	29
$SO_4^{2-} + H^+ = HSO_4^-$	1.06 ± 0.02	25.0	cplx	*b*
	1.10[e]	25	pH	30
$H_2PO_3^- + H^+ = H_3PO_3$	1.01 ± 0.01	10.0	cplx	*b*
	0.97[d]	25.0	pH	29
$HPO_3^- + H^+ = H_2PO_3^-$	6.34 ± 0.07	10.0	UV−vis	*b*
	6.70[c]	20.0	pH	31
$H_2AsO_3^- + H^+ = H_3AsO_3$	9.23[c]	18	pH	27
$Fe^{3+} + SO_4^{2-} = FeSO_4^+$ (K_{sul})	2.06 ± 0.01	25.0	UV−vis	*b*
	2.31[f]	25.0	UV−vis	32
$Fe^{3+} + H_2PO_2^- = FeH_2PO_2^{2+}$	2.81 ± 0.01	10.0	UV−vis	*b*
	3.04[d]	25.0	kin	29
$Fe^{3+} + H_2PO_3^- = FeH_2PO_3^{2+}$	2.69 ± 0.04	10.0	UV−vis	*b*
	5.0	24	pot.	33
$Fe^{3+} + H_2AsO_4^- = FeH_2AsO_4^{2+}$	2.64 ± 0.02	10.0	UV−vis	*b*
$Fe^{3+} + HSeO_3^- = FeHSeO_3^{2+}$	3.15 ± 0.01	10.0	UV−vis	*b*
	3.25	20	UV−vis	34

[a] pH, pH-potentiometry; UV−vis, UV−vis spectrophotometry; est, estimated on the basis of the value measured at 25.0 °C and the standard enthalpy of reaction; cplx, determined from the equilibrium complexation study with monomeric Fe(III) using UV−vis spectrophotometry; kin, estimated from kinetic results; pot., potentiometry of the Fe(II)/Fe(III) system. [b] This work. [c] Extrapolated to μ = 0. [d] μ = 1.0 M ($LiNO_3$). [e] μ = 1.0 M ($NaNO_3$). [f] μ = 0.5 M ($NaClO_4$).

Table 2. Rate Constants for the Hydrolytic Reactions of Iron(III); μ = 1.0 M ($NaClO_4$)

parameter	value at 25.0 °C (ref 6)	value at 10.0 °C (ref 11)
k_1	0.35 s^{-1}	0.059 s^{-1}
k_2	3.5 $M^{-1}s^{-1}$	1.08 $M^{-1}s^{-1}$
k_3	3.6×10^{-3} $M\,s^{-1}$	5.8×10^{-4} $M\,s^{-1}$
k_{-1}	1.3×10^2 $M^{-1}s^{-1}$	71 $M^{-1}s^{-1}$
k_{-2}	2.5 $M^{-1}s^{-1}$	1.2 $M^{-1}s^{-1}$
k_{-3}	6.7×10^3 $M^{-1}s^{-1}$	3.3×10^3 $M^{-1}s^{-1}$

and the pseudo-first-order rate constant, k_{hdr}, can be expressed as[6]

$$k_{hdr} = k_h + 4k_{-h}[Fe_{mn}] \tag{5}$$

where $[Fe_{mn}] = [Fe^{3+}] + [FeOH^{2+}] + [Fe(OH)_2{}^+]$, and k_h and k_{-h} are given as follows:[6]

$$k_h = k_1 + k_2[H^+] + \frac{k_3}{[H^+]} \tag{6}$$

$$k_{-h} = \frac{\beta_1}{(\beta_1 + [H^+] + \beta_2/[H^+])^2}\left(k_{-1}\beta_1 + k_{-2}[H^+] + \frac{k_{-3}\beta_2}{[H^+]}\right) \tag{7}$$

Rate constants k_1, k_2, k_3, k_{-1}, k_{-2}, and k_{-3} are listed in Table 2.[6,11]

The protonation constants of the ligands ($K_p = [H_nL]/[H_{n-1}L]/[H^+]$) for the conditions of this study were deter-

(17) Fábián, I.; Gordon, G. *Inorg. Chem.* **1991**, *30*, 3994.
(18) Fábián, I.; Gordon, G. *Inorg. Chem.* **1992**, *31*, 2144.
(19) Everett, K. G.; Skoog, D. A. *Anal. Chem.* **1971**, *43*, 1541.
(20) Tonomura, B.; Nakatani, H.; Ohnishi, M.; Yamaguchi-Ito, J.; Hiromi, K. *Anal. Biochem.* **1978**, *84*, 370.
(21) Pócsi, I.; Fábián, I. *J. Chem. Soc., Dalton Trans.* **1988**, 2231.
(22) Zékány, L.; Nagypál, I. In *Computational Methods for the Determination of Formation Constants*; Legett, D. J., Ed.; Plenum Press: New York, 1985; p 291.
(23) *SCIENTIST*, version 2.01; Micromath Software: Salt Lake City, UT, 1995.

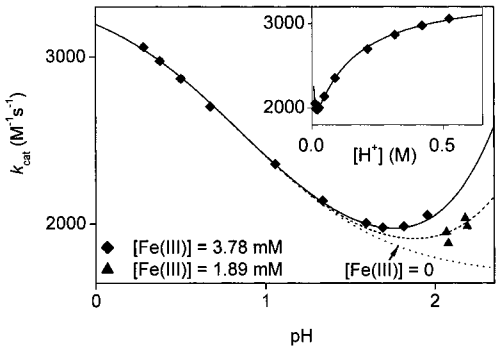

Figure 1. Value of k_{cat} as a function of pH in the iron(III)−arsenite ion system. Inset: k_{cat} as a function of $[H^+]$. $T = 25.0$ °C; $\mu = 1.0$ M ($NaClO_4$). Lines represent the best fit to eq 13.

mined using pH-potentiometry and UV−vis spectrophotometry (Table 1).[27−34]

Redox Reactions. The possibility of redox reactions between iron(III) and some of the ligands (H_3AsO_3, H_3PO_2, H_3PO_3, H_2SeO_3) was tested at room temperature by monitoring the buildup of iron(II) with a spectrophotometric method using 2,2′-dipyridyl. Formation of iron(II) was not detected in any of the reactions up to 45 min. These results confirm that the redox reactions are very slow and do not interfere with the ligand substitution reactions, which are complete in a few minutes at 10.0 °C.

Arsenic(III) Catalyzed Hydrolytic Reactions. Iron(III) solutions have the same UV−vis spectra in the presence and absence of arsenite ion; that is, complex formation between iron(III) and As(III) cannot be detected by spectrophotometry. Nevertheless, the dissociation of $Fe_2(OH)_2^{4+}$ upon mixing with an acid solution becomes faster in the presence of As(III). The characteristic first-order kinetic traces at 340 nm are identical, regardless of whether arsenite ion is initially added to the iron(III) or to the acid solution, confirming that stable complexes, which would certainly affect the dissociation rate of $Fe_2(OH)_2^{4+}$ in the first case, do not form between the reactants.

At constant pH, k_{obs} is a linear function of the concentration of arsenite ion:

$$k_{obs} = k_{hdr} + k_{cat}[\mathrm{As(III)}] \qquad (8)$$

where k_{hdr} is given in eq 5 and k_{cat} corresponds to the catalytic path. The value for k_{obs} was found to be slightly dependent on total iron(III) concentration above pH 1.7, and k_{cat} is a composite function of pH (Figure 1) as it reaches some kind of limiting value at high acidities, has a minimum at about pH 1.8, and rises again at lower acidities. The shape of the curve in Figure 1 indicates that at least two catalytic pathways are operative. However, the observed pH dependence cannot be assigned to any known protolytic equilibrium which involves the reactants. The lowest log K_p for arsenite ion ($H_2AsO_3^- + H^+ = H_3AsO_3$) was reported to be 9.23.[35−37] The main hydrolytic reaction of iron(III) is the formation of $FeOH^{2+}$ in this pH range, but the observed effect cannot be assigned to this process because it would predict a markedly different pH profile of k_{cat}.

It might be argued that the difference between the lowest and highest k_{cat} values is only about 50%, and some of the change might be due to a variation in the medium because at high acidities significantly smaller amounts of $NaClO_4$ are used to set the ionic strength. This possibility was tested by two series of experiments: the first with always 1.00 M $NaClO_4$ added, that is, $\mu > 1.0$ M at high acidities, and the second with smaller amounts of $NaClO_4$ to set the ionic strength exactly to 1.00 M. The corresponding rate constants agreed within 5%, confirming that medium effects do not contribute to the noted pH dependence of k_{cat}.

The catalytic effect implies a direct interaction between the $Fe_2(OH)_2^{4+}$ and the arsenite ion. In accordance with previous results,[6,10−14,16] we assume that a dinuclear complex is formed:

$$Fe_2(OH)_2^{4+} + H_3AsO_3 \rightleftharpoons Fe_2As^{III}$$

$$v_9 = k_9[Fe_2(OH)_2^{4+}][H_3AsO_3] - k_{-9}[Fe_2As^{III}] \qquad (9)$$

While Fe_2As^{III} is not formed in detectable concentrations, it may open a catalytic pathway for the hydrolytic reaction via fast dissociation into mononuclear iron(III) species. The pH dependence of k_{cat} strongly suggests that the dinuclear arsenito complex undergoes direct and proton-assisted dissociation.

$$Fe_2As^{III} \rightleftharpoons FeOH^{2+} + FeAs^{III}$$

$$v_{10} = k_{10}[Fe_2As^{III}] - k_{-10}[FeOH^{2+}][FeAs^{III}] \qquad (10)$$

$$Fe_2As^{III} + H^+ \rightleftharpoons Fe^{3+} + FeAs^{III}$$

$$v_{11} = k_{11}[Fe_2As^{III}][H^+] - k_{-11}[Fe^{3+}][FeAs^{III}] \qquad (11)$$

The scheme is completed by the dissociation of the mononuclear arsenito complex, $FeAs^{III}$, which is always present at very low concentration levels. To be able to coordinate to the metal ion, H_3AsO_3 needs to release at least one proton, and the corresponding reaction can be written as

(24) Lente, G.; Jacob, J.; Guzei, I. A.; Espenson, J. H. *Inorg. React. Mech. (Amsterdam)* **2000**, *2*, 169.
(25) Nemes, A.; Fábián, I. Gordon, G. *Inorg. React. Mech. (Amsterdam)* **2001**, *2*, 327.
(26) Tóth, Zs.; Fábián, I. *Inorg. Chem.* **2000**, *39*, 4608.
(27) Britton, H. T. S.; Jackson, P. *J. Chem. Soc.* **1934**, 1048.
(28) Arnek, R.; Barcza, L. *Acta Chem. Scand.* **1972**, *26*, 213.
(29) Espenson, J. H.; Dustin, D. F. *Inorg. Chem.* **1969**, *8*, 1760.
(30) Khoe, G. H.; Robins, R. G. *J. Chem. Soc., Dalton Trans.* **1988**, 2015.
(31) Frei, V.; Podlahová, J.; Podlaha, J. *Collect. Czech. Chem. Commun.* **1964**, *29*, 2587.
(32) Davis, G. G.; Smith, W. MacF. *Can. J. Chem.* **1962**, *40*, 1836.
(33) Masalovich, V. M.; Agasyan, P. K.; Nikolaeva, E. R. *Zh. Neorg. Khim.* **1966**, *11*, 272.
(34) Hamada, S.; Ishikawa, Y.; Shirai, T. *Nippon Kagaku Zasshi* **1965**, *86*, 1042.

(35) The structures of H_3AsO_3 and $H_2AsO_3^-$ are better expressed by the formulas $As(OH)_3$ and $AsO(OH)_2^-$, respectively (see ref 37). However, as no structural conclusions are drawn in this work and the structures in the metal complexes are not necessarily the same as in the free ligand, the simplified formulas were chosen to indicate the overall composition only.

(36) Sellers, P.; Sunner, S.; Wadsö, I. *Acta Chem. Scand.* **1964**, *18*, 202.
(37) Loehr, T. M.; Plane, R. A. *Inorg. Chem.* **1968**, *7*, 1708.

$$Fe^{3+} + H_3AsO_3 \rightleftharpoons FeAs^{III} + H^+ \quad K_{12} = \frac{[FeAs^{III}][H^+]}{[Fe^{3+}]\,[H_3AsO_3]} \tag{12}$$

Provided that reaction 12 is fast and steady-state applies to Fe_2As^{III}, standard derivation yields the following expression for k_{cat}:[38]

$$k_{cat} = \frac{k_9k_{10}/k_{11} + k_9[H^+]}{(k_{-9} + k_{10})/k_{11} + [H^+]} + \frac{4[Fe_{mn}]((k_{-9}k_{-10}/k_{11})\beta_1K_{12} + (k_{-9}k_{-11}/k_{11})K_{12}[H^+])}{(\beta_1 + [H^+] + \beta_2/[H^+]^2)\,((k_{-9} + k_{10})/k_{11} + [H^+])} \tag{13}$$

Considering microscopic reversibility, $k_{-9}k_{-10}\beta_1K_{12}$ and $k_{-9}k_{-11}K_{12}$ can be replaced by $k_9k_{10}\beta_3$ and $k_9k_{11}\beta_3$, respectively. The fitted values for the three remaining independent parameters, k_9, k_9k_{10}/k_{11}, and $(k_{-9} + k_{10})/k_{11}$ are listed in Table 3.[39]

Formation Kinetics of Mononuclear Iron(III) Complexes. The dominant final products are always mononuclear iron(III) complexes ($FeH_2PO_3^{2+}$, $FeH_2PO_2^{2+}$, $FeH_2AsO_4^{2+}$, $FeSO_4^+$, and $FeHSeO_3^{2+}$) in the rest of reactions studied here. Experiments were carried out to determine the equilibrium and kinetic parameters for the formation of the mononuclear complexes under conditions where the reactions of $Fe_2(OH)_2^{4+}$ could be neglected ($[Fe(III)]_{tot} < 0.2$ mM). Numerous stability constants are available from the literature for mononuclear complexes,[29,32−34] and kinetic data were also reported with sulfate and hypophosphite ions.[29,32] Thus, we performed routine measurements to redetermine equilibrium and rate constants for our conditions, and these studies are not discussed in detail. The equilibrium results are summarized in Table 1, and the kinetic data were evaluated in terms of the following scheme:

$$Fe^{3+} + HL \rightleftharpoons FeL^{2+} + H^+$$

$$v_{14} = k_{14}[Fe^{3+}][HL] - k_{-14}[FeL^{2+}][H^+] \tag{14}$$

$$Fe(OH)^{2+} + HL \rightleftharpoons FeL^{2+}$$

$$v_{15} = k_{15}[FeOH^{2+}][HL] - k_{-15}[FeL^{2+}] \tag{15}$$

$$Fe^{3+} + L^- \rightleftharpoons FeL^{2+}$$

$$v_{16} = k_{16}[Fe^{3+}][L^-] - k_{-16}[FeL^{2+}] \tag{16}$$

$$Fe(OH)^{2+} + L^- \rightleftharpoons FeL^{2+}$$

$$v_{17} = k_{17}[FeOH^{2+}][L^-] - k_{-17}[FeL^{2+}]/[H^+] \tag{17}$$

where $L^- = SO_4^{2-}$, $H_2PO_2^-$, $H_2PO_3^-$, $H_2AsO_4^-$, and $HSeO_3^-$. Protolytic reactions of the ligand are expected to be diffusion controlled, and reactions 15 and 16 are indistinguishable because of proton ambiguity. Thus, only the appropriate combination of equilibrium and rate constants ($k_{15}\beta_1K_p + k_{16}$) could be determined. The results are listed in Table 4.

(38) A treatment involving steady-state approach for both $FeAs^{III}$ and Fe_2As^{III} also yields eq 13.

Table 3. Parameters Determined for the Iron(III)−Arsenic(III) and Sulfate Ion Reactions; 25.0 °C, μ = 1.0 M ($NaClO_4$)

ligand	parameter	value
H_3AsO_3	k_9	$(3.43 \pm 0.03) \times 10^3$ M^{-1} s^{-1}
	k_9k_{10}/k_{11}	$(2.5 \pm 0.1) \times 10^2$ s^{-1}
	$(k_{-9} + k_{10})/k_{11}$	0.149 ± 0.008 M
	$K_{12}k_{-9}k_{-10}/k_{11}$	1.8×10^2 s^{-1}[a]
	$K_{12}k_{-9}k_{-11}/k_{11}$	4.7 s^{-1}[b]
SO_4^{2-}	K_{18}	$(6.0 \pm 0.1) \times 10^2$ M^{-1}
	k_{19}	4.60 ± 0.06 s^{-1}
	k_{-19}	200 M^{-1} s^{-1}[c]
	$\epsilon\{FeSO_4^+\}$, 340 nm	1811 ± 8 M^{-1} cm^{-1}

[a] Replaced by $(k_9k_{10}/k_{11}) \times \beta_3/\beta_1$ in the calculations. [b] Replaced by $k_9\beta_3$ in the calculations. [c] Replaced by $k_{19}\beta_3K_{18}K_p/(\beta_1K_{MS})$ in the calculations.

Table 4. Rate Constants (in M^{-1} s^{-1}) for the Formation Reactions of Monomeric Complexes of Iron(III); μ = 1.0 M ($NaClO_4$)

L^-	k_{14}	$k_{15}\beta_1K_p + k_{16}$	k_{17}	T (°C)
SO_4^{2-}	*a*	$(2.4 \pm 0.3) \times 10^3$	$(6.6 \pm 0.5) \times 10^4$	25.0
$H_2PO_2^-$	5.9 ± 1.3	13 ± 2	$(1.7 \pm 0.1) \times 10^3$	10.0
$H_2PO_3^-$	*a*	33 ± 7	$(1.9 \pm 0.1) \times 10^3$	10.0
$H_2AsO_4^-$	2.0 ± 0.7	65 ± 10	$(2.5 \pm 0.1) \times 10^3$	10.0
$HSeO_3^-$	*a*	$(1.71 \pm 0.03) \times 10^3$	$(1.1 \pm 0.1) \times 10^4$	10.0

[a] Too small to be determined.

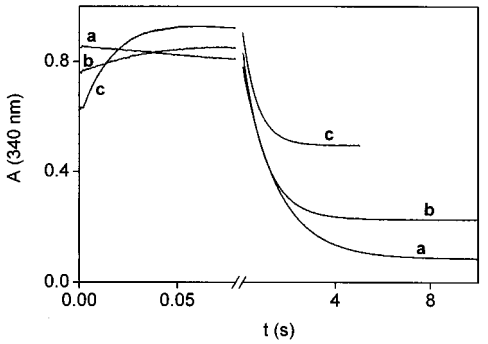

Figure 2. Kinetic traces in the iron(III)−sulfate ion system. [Fe(III)] = 3.00×10^{-3} M; $[SO_4^{2-}]_T$ = 0 (a), 5.0×10^{-4} M (b), 1.5×10^{-3} M (c); pH = 1.12; T = 25.0 °C; μ = 1.0 M ($NaClO_4$); optical path length 1 cm.

Sulfate Ion−Iron(III) System. Sulfate ion decreases the initial absorbance of the kinetic curves considerably (Figure 2). This effect is consistent with a reaction within the dead time of the stopped flow instrument (phase I), which was immeasurably fast even at 5.0 °C irrespective of the initial concentrations. According to our independent experiments (cf. previous section), no reaction occurs with monomeric iron(III) within this short time frame, and a detailed analysis of the data confirmed that the initial absorbance jump corresponds to a reaction between $Fe_2(OH)_2^{4+}$ and sulfate ion. The amplitude of the absorbance jump decreases with increasing pH and correlates well with the shift in the HSO_4^-/SO_4^{2-} protolytic equilibrium. All experimental data could be interpreted assuming the formation of a dinuclear complex which has no measurable absorbance at 340 nm:

$$Fe_2(OH)_2^{4+} + HSO_4^- \rightleftharpoons Fe_2(OH)SO_4^{3+} (+ H_2O)$$

$$K_{18} = \frac{[Fe_2(OH)SO_4^{3+}]}{[Fe_2(OH)_2^{4+}][HSO_4^-]} \tag{18}$$

The value of K_{18} is given in Table 3.

As seen in Figure 2, there are two additional distinct phases (phase II ~ 0.05 s, and phase III ~ 5 s) during the process. The absorbance increase in phase II was consistent with the formation of $FeSO_4^+$, and the kinetic parameters estimated from these experiments are in excellent agreement with results obtained independently at ligand excess and low iron(III) concentration.

Phase III could be interpreted as equilibration between mononuclear and dinuclear hydroxo complexes of iron(III). The kinetic curves in this phase were always strictly first-order, but the pseudo-first-order rate constants were systematically and significantly larger than the corresponding k_{hdr} values, indicating that sulfate ion also catalyzes the hydrolytic reactions of iron(III). This catalytic effect can be interpreted in analogy with the arsenic catalysis by replacing reactions 10 and 11 with reaction 19 in the model:

$$Fe_2(OH)SO_4^{3+} \rightleftharpoons FeOH^{2+} + FeSO_4^+$$

$$v_{19} = k_{19}[Fe_2(OH)SO_4^{3+}] - k_{-19}[FeOH^{2+}][FeSO_4^+] \quad (19)$$

In this system, proton-assisted dissociation of $Fe_2(OH)SO_4^{3+}$ (cf. reaction 11) has a negligible contribution to the overall rate, if it occurs at all. Thus k_{obs} can be expressed as follows:

$$k_{obs} = k_f + 4k_r[Fe_{mn}] \quad (20)$$

where k_f and k_r are

$$k_f = \frac{k_h(1 + K_p[H^+]) + k_{19}K_{18}K_p[S(VI)]_{free}[H^+]}{1 + K_p[H^+] + K_{18}K_p[S(VI)]_{free}[H^+]} \quad (21)$$

$$k_r = k_{-h} + \frac{k_{-19}K_{sul}\beta_1[S(VI)]_{free}[H^+]}{(1 + K_p[H^+])(\beta_1 + [H^+] + \beta_2/[H^+])^2} \quad (22)$$

where $[S(VI)]_{free}$ is the concentration of free sulfate ion ($[HSO_4^-] + [SO_4^{2-}]$)[40] and K_{sul} is the stability constant of $FeSO_4^+$ (cf. Table 1). The value of $[S(VI)]_{free}$ was calculated from the known equilibrium constants for each point, and k_{-19} was replaced by $k_{19}\beta_3K_{18}K_p/(\beta_1K_{sul})$ considering microscopic reversibility in the fitting procedure. The results are listed in Table 3, and the fit of the experimental data is illustrated in Figure 3.

Reactions of Iron(III) with Arsenate, Selenite, Phosphite, and Hypophosphite Ions. As an example, kinetic curves are shown for the arsenate ion system at two wavelengths in Figure 4. Similar biphasic kinetic traces were observed with each of the other ligands. The initial absorbance was independent of the ligand concentration, and any reaction within the dead time of the stopped-flow instrument could be excluded. The first phase of the reaction was complete

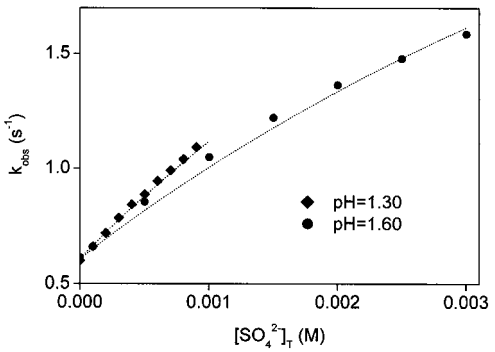

Figure 3. Value of k_{obs} as a function of sulfate ion concentration in the iron(III)−sulfate ion system. Dashed lines represent the best fit to eq 20. $[Fe(III)] = 5.00 \times 10^{-3}$ M for pH = 1.30; $[Fe(III)] = 3.00 \times 10^{-3}$ M for pH = 1.60; $T = 25.0$ °C; $\mu = 1.0$ M ($NaClO_4$).

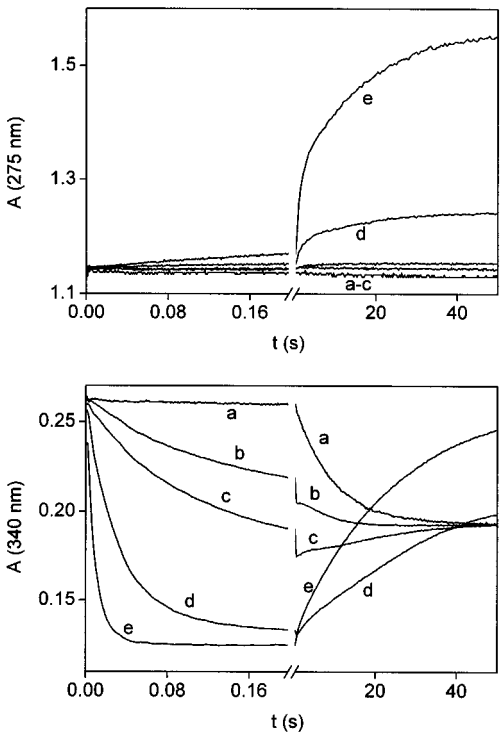

Figure 4. Kinetic traces in the iron(III)−arsenate ion system. $[Fe(III)] = 4.50 \times 10^{-3}$ M; $[Fe_2(OH)_2^{4+}]_0 = 5.0 \times 10^{-5}$ M; [As(V)] = 0 (a), 2.5×10^{-5} M (b), 5.0×10^{-5} M (c), 2.5×10^{-4} M (d), 1.0×10^{-3} M (e); pH = 1.60; $T = 10.0$ °C; $\mu = 1.0$ M ($NaClO_4$); optical path length 2 mm (275 nm), 1 cm (340 nm).

in about 0.1 s, whereas the second usually lasted 10−50 s. The initial rate method confirmed the following rate equation for phase I in each system:

$$v_i = k_d[Fe_2(OH)_2^{4+}][L]_T \quad (23)$$

where $[L]_T = [HL] + [L^-]$ and $L^- = H_2PO_2^-$, $H_2PO_3^-$, $H_2AsO_4^-$, $HSeO_3^-$.

The lack of significant absorbance change at the characteristic absorption band of $FeH_2AsO_4^{2+}$ (275 nm) rules out excessive formation of this complex in Phase I, and the observations at 340 nm are consistent with the formation of a new complex. The very same conclusion can be drawn for the reactions of selenite, phosphite, and hypophosphite ions.

The composition of the product formed in phase I was tested by analyzing the amplitude of the absorbance change

(39) A fitting was attempted by calculating five independent parameters (k_9, k_9k_{10}/k_{11}, $(k_{-9} + k_{10})/k_{11}$, $k_{-9}k_{-10}/k_{11}$, and $k_{-9}k_{-11}/k_{11}$), but this did not give satisfactory results because of irresolvable cross correlation between the parameters.

(40) The main sulfur(VI)-containing species in this system are free sulfate ion and the mononuclear complex $FeSO_4^+$ (the concentration of $Fe_2(OH)SO_4^{3+}$ is much smaller). The equilibrium between the two major forms are reached by the end of phase II, and the concentration of free sulfate remains practically constant throughout phase III.

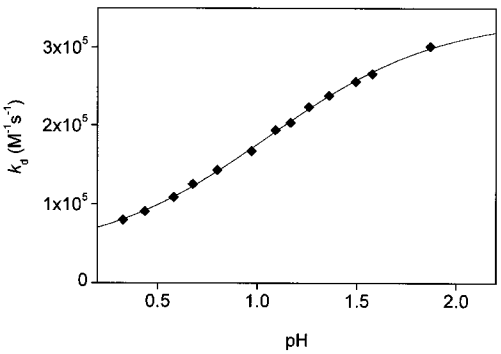

Figure 5. Value of k_d as a function of pH in the iron(III)−phosphite ion system. The solid line represents the best fit to eq 26. $T = 10.0$ °C; $\mu = 1.0$ M ($NaClO_4$).

in phase I with phosphite and arsenate ions. This method could not be used with selenite and hypophosphite ions because of overlapping subsequent reactions. Similarly to the reaction with phosphate ion,[11] a 1:2 stoichiometry was confirmed for As(V) and $Fe_2(OH)_2^{4+}$ in the new complex (Fe_4L) by the molar ratio as well as the Job methods.[41] The same treatment proved the formation of a 1:1 complex (Fe_2L) between P(III) and $Fe_2(OH)_2^{4+}$ in the phosphite ion system. These complexes have negligible absorption at 340 nm. In analogy, selenite and hypophosphite ions were assumed to form 1:1 complexes with $Fe_2(OH)_2^{4+}$.

The pH dependence of the formation of Fe_2L with phosphite ion could be studied under pseudo-first-order conditions using phosphite ion in 15-fold excess over $Fe_2(OH)_2^{4+}$. These conditions ensured that the reverse reaction was negligible and the forward rate constant k_d could be calculated from k_{obs}. As expected, the two protonated forms, H_3PO_3 and $H_2PO_3^-$, show different reactivities (Figure 5), and the two pathways for the formation of Fe_2L ($L^- = H_2PO_3^-$) are as follows:

$$Fe_2(OH)_2^{4+} + HL = Fe_2L + H^+$$

$$v_{24f} = k_{24}[Fe_2(OH)_2^{4+}][HL] \quad (24)$$

$$Fe_2(OH)_2^{4+} + L^- = Fe_2L$$

$$v_{25f} = k_{25}[Fe_2(OH)_2^{4+}][L^-] \quad (25)$$

The proton budgets of these reactions were confirmed by the combination of the pH dependences of the forward and reverse rates (see later). The following formula can be derived for k_d:

$$k_d = \frac{k_{25} + k_{24}K_p[H^+]}{1 + K_p[H^+]} \quad (26)$$

The same kind of pseudo-first-order studies were not possible with $H_2PO_2^-$, $H_2AsO_4^-$, and $HSeO_3^-$. In these cases, the pH-dependence of the forward rates was studied by the initial rate method, which indicated a pH dependence similar to the one observed with phosphite ion. However, in the case of hypophosphite ion, the proton budget of the reaction was different (see later). The corresponding rate constants were calculated assuming that the complexes have no absorptions at the wavelength used (340 nm for arsenate and hypophosphite ions, 370 nm for selenite ion). This assumption was fully confirmed later with detailed model calculations and matrix rank analysis. The results are summarized in Table 5.

Table 5. Forward Rate Constants for the Formation of Fe_2L Complexes with Various Forms of Simple Inorganic Ligands; 10.0 °C, $\mu = 1.0$ M ($NaClO_4$)

ligand (H_nL)	k (M^{-1} s^{-1})			ref
	H_nL	$H_{n-1}L^-$	$H_{n-2}L^{2-}$	
H_3PO_2	$(2.9 \pm 0.1) \times 10^4$	$(3.49 \pm 0.02) \times 10^5$		*a*
H_3PO_3	$(3.3 \pm 0.3) \times 10^4$	$(3.40 \pm 0.03) \times 10^5$		*a*
H_3PO_4	$< 1 \times 10^4$	1.44×10^5		11
H_3AsO_3	$(3.43 \pm 0.03) \times 10^{3b}$			*a*
H_3AsO_4	$(8 \pm 2) \times 10^3$	$(2.5 \pm 0.1) \times 10^5$		*a*
$H_2O{\cdot}SO_2$	$< 5 \times 10^3$	4.5×10^4	2.1×10^9	10
H_2SO_4		n.d[c]	$>1.0 \times 10^7$	*a*
H_2SeO_3	$(2.7 \pm 0.1) \times 10^4$	$(4.6 \pm 0.2) \times 10^5$		*a*

[a] This work. [b] 25.0 °C. [c] No data; any value below 10^6 M^{-1} s^{-1} is consistent with the data.

The complex kinetic patterns observed in phase II were interpreted as simultaneous formation of mononuclear iron(III) complexes and a shift in the iron(III) hydrolytic equilibria. This phase was evaluated on the basis of the following kinetic model:

$$Fe_2(OH)_2^{4+} + L' \rightleftharpoons Fe_2L$$

$$v = k_d[Fe_2(OH)_2^{4+}][L]_T - k_{-d}[Fe_2L] \quad (27)$$

$$Fe_2L \rightleftharpoons FeL + Fe_{mn}$$

$$v = k_s[Fe_2L] - k_{-s}[FeL][Fe_{mn}] \quad (28)$$

$$Fe_{mn} + L' \rightleftharpoons FeL$$

$$v = k_m[Fe_{mn}][L]_T - k_{-m}[FeL] \quad (29)$$

$$Fe_2(OH)_2^{4+} \rightleftharpoons 2Fe_{mn}$$

$$v = k_h[Fe_2(OH)_2^{4+}] - k_{-h}[Fe_{mn}]^2 \quad (30)$$

where L′ denotes the general form of the ligand and $[L]_T = [HL] + [L^-]$.

In these calculations, all rate constants known from separate studies (cf. previous sections) were fixed, and colored species were included with molar absorbance coefficients determined in independent measurements. Protolytic equilibria of the ligands and mononuclear iron(III) species were considered as fast preequilibria. The values of k_{-d} and k_s were fitted, while k_{-s} was replaced with $k_s k_d k_{-m} k_{-h}/(k_{-d} k_m k_h)$ on the basis of microscopic reversibility. As expected, none of the rate constants was dependent on the initial iron(III) (monomeric or dimeric) or ligand concentrations, but some of them showed distinct pH dependences.

In the case of selenite ion, k_{-d} increased slightly with increasing acidity. This is consistent with eqs 24 and 25 as the reverse rates of the corresponding reactions can be given as

$$v_{24r} = k_{-24}[Fe_2L][H^+] \quad (31)$$

$$v_{25r} = k_{-25}[Fe_2L] \quad (32)$$

(41) Job, P. *Ann. Chim.* **1928**, *9*, 113.

and k_{-d} can be expressed as

$$k_{-d} = k_{-24}[H^+] + k_{-25} \quad (33)$$

The value of k_s also increases linearly with $[H^+]$. This implies a direct and a proton-assisted pathway in the dissociation of Fe_2L:

$$Fe_2L = Fe(OH)_2^{+} + FeHL^{2+}$$

$$v_{34} = k_{34}[Fe_2L] - k_{-34}[Fe(OH)_2^{+}][FeHL^{2+}] \quad (34)$$

$$Fe_2L + H^+ = Fe(OH)^{2+} + FeHL^{2+}$$

$$v_{35} = k_{35}[Fe_2L][H^+] - k_{-35}[Fe(OH)^{2+}][FeHL^{2+}] \quad (35)$$

Thus, k_s is given as

$$k_s = k_{34} + k_{35}[H^+] \quad (36)$$

In the phosphite ion system, k_{-d} was too small and could not be determined directly. Consequently, k_{-d} was set to zero, and k_{-s} was determined as an independent parameter. The value of k_s was found to be independent of pH, indicating that reaction 34 is the dominant path in the dissociation of the dinuclear complex. It follows that $k_s = k_{34}$ and $k_{-s} = k_{-34}\beta_2/([H^+]^2 + \beta_1[H^+] + \beta_2)$, provided that the formula of Fe_2L is $Fe_2(OH)(HPO_3)^{3+}$.

In the case of hypophosphite ion, k_{-d} increased with increasing pH. Considering that the forward rate shows the same pH dependence as for the other ligands, this pH dependence could only be interpreted by the following scheme, assuming that the complex Fe_2L has the stoichiometry $Fe_2OH(H_2PO_2)^{4+}$:

$$Fe_2(OH)_2^{4+} + H_3PO_2 = Fe_2(OH)(H_2PO_2)^{4+}$$

$$v_{37} = k_{37}[Fe_2(OH)_2^{4+}][H_3PO_2] - k_{-37}[Fe_2(OH)(H_2PO_2)^{4+}] \quad (37)$$

$$Fe_2(OH)_2^{4+} + H_2PO_2^{-} + H^+ = Fe_2(OH)(H_2PO_2)^{4+}$$

$$v_{38} = k_{38}[Fe_2(OH)_2^{4+}][H_2PO_2^{-}] - k_{-38}[Fe_2(OH)(H_2PO_2)^{4+}]/[H^+] \quad (38)$$

$$k_{-d} = k_{-37} + k_{-38}/[H^+] \quad (39)$$

The pH dependence of k_s is similar to that of k_{-d} and consistent with the following scheme:

$$Fe_2(OH)(H_2PO_2)^{4+} = FeOH^{2+} + Fe(H_2PO_2)^{2+}$$

$$v_{40} = k_{40}[Fe_2(OH)(H_2PO_2)^{4+}] - k_{-40}[FeOH^{2+}][Fe(H_2PO_2)^{2+}] \quad (40)$$

$$Fe_2(OH)(H_2PO_2)^{4+} = Fe(OH)_2^{+} + Fe(H_2PO_2)^{2+} + H^+$$

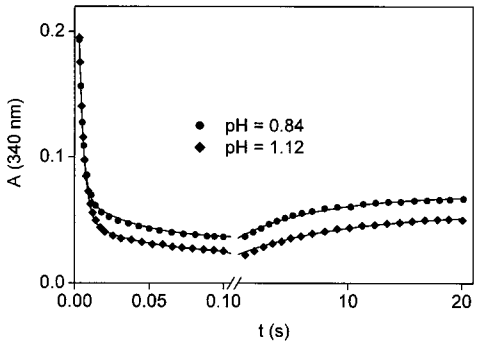

Figure 6. Measured (markers) and fitted (solid lines) kinetic curves in the iron(III)−hypophosphite ion system. $[Fe(III)] = 2.59 \times 10^{-3}$ M; $[P(I)] = 1.5 \times 10^{-3}$ M; $T = 10.0$ °C; $\mu = 1.0$ M ($NaClO_4$); optical path length 1 cm. Only a selection (~10%) of measured points is shown for clarity.

$$v_{41} = k_{41}[Fe_2(OH)(H_2PO_2)^{4+}]/[H^+] - k_{-41}[Fe(OH)_2^{+}][Fe(H_2PO_2)^{2+}] \quad (41)$$

$$k_s = k_{40} + k_{41}/[H^+] \quad (42)$$

Kinetic curves could be fitted reasonably to this model (Figure 6).

The arsenate ion system was found to be very similar to the one reported for phosphate ion, and the same evaluation method was used.[11] Reaction 28 was found to be negligible, and one more step was added to the model used for the previous systems in order to account for the formation of the Fe_4L complex:

$$Fe_2As + Fe_2(OH)_2^{4+} = Fe_4As$$

$$K_{43} = \frac{[Fe_4As]}{[Fe_2(OH)_2^{4+}][Fe_2As]} \quad (43)$$

Reaction 43 is too fast on the stopped-flow time scale; only its equilibrium constant could be determined. It can be shown that Fe_2As is present at very low concentration levels during the formation of Fe_4As, which is the dominant multinuclear arsenato species. These findings also explain the first-order dependence of phase I on the concentration of $Fe_2(OH)_2^{4+}$ because reaction 27 is rate determining in the formation of Fe_4As. In full analogy with the phosphate ion system,[11] the stoichiometries $Fe_2(HAsO_4)(OH)^{3+}$ and $Fe_4(AsO_4)(OH)_2^{7+}$ were confirmed for Fe_2As and Fe_4As, respectively. The results for these systems are collected in Table 6.

Matrix rank analysis (MRA)[42] was used to find further support for the kinetic models proposed here. MRA confirms the existence of 3 major absorbing species (Fe^{3+}, $FeOH^{2+}$, and $Fe_2(OH)_2^{4+}$) in an iron(III) solution in the absence of ligands. During the complex formation reactions, one additional absorbing species is detectable, which is the monomeric iron(III) complex in each case ($FeH_2PO_3^{2+}$, $FeH_2PO_2^{2+}$, $FeH_2AsO_4^{2+}$, and $FeHSeO_3^{2+}$). Thus, in agreement with our considerations, the multinuclear complexes do not

(42) Peintler, G.; Nagypál, I.; Jancsó, A.; Epstein, I. R.; Kustin, K. *J. Phys. Chem. A* **1997**, *101*, 8013.

Table 6. Parameters Determined or Used in Kinetic Modeling; 10.0 °C, $\mu = 1.0$ M ($NaClO_4$)[a]

phosphite ion	hypophosphite ion	selenite ion	arsenate ion
$k_{34} = 0.18 \pm 0.04\ s^{-1}$	$k_{-37} = 4.4 \pm 0.06\ s^{-1}$	$k_{-24} = 14 \pm 7\ M^{-1}\,s^{-1}$	$K_{43} = (6 \pm 2) \times 10^4\ M^{-1}\,s^{-1}$
$k_{-34} = 81 \pm 15\ M^{-1}\,s^{-1}$	$k_{-38} = 2.9 \pm 0.1\ M\ s^{-1}$	$k_{-25} = 26 \pm 1\ s^{-1}$	$k_{-24} = 26 \pm 3\ M^{-1}\,s^{-1}$
	$k_{40} = 19 \pm 3\ s^{-1}$	$k_{34} = 0.64 \pm 0.04\ s^{-1}$	$k_{-25} = 108 \pm 16\ s^{-1}$
	$k_{41} = 2.06 \pm 0.09\ M\ s^{-1}$	$k_{35} = 6.8 \pm 0.4\ M^{-1}\ s^{-1}$	
$\epsilon\{FeH_2PO_3^{2+}\}_{340nm}$	$\epsilon\{FeH_2PO_2^{2+}\}_{340nm}$	$\epsilon\{FeHSeO_3^{2+}\}_{370nm}$	$\epsilon\{FeH_2AsO_4^{2+}\}_{340nm}$
$235 \pm 14\ M^{-1}\,cm^{-}$	$70 \pm 1\ M^{-1}\,cm^{-1}$	$527 \pm 20\ M^{-1}\,cm^{-1}$	$460 \pm 50\ M^{-1}\,cm^{-1}$

$\epsilon\{Fe_2(OH)_2^{4+}\}_{340nm}$ 2760 $M^{-1}\,cm^{-1}$ (ref 11)
$\epsilon\{Fe_2(OH)_2^{4+}\}_{370nm}$ 630 $M^{-1}\,cm^{-1}$ (ref 11)
$\epsilon\{FeOH^{2+}\}_{340nm}$ 700 $M^{-1}\,cm^{-1}$ (ref 11)
$\epsilon\{FeOH^{2+}\}_{370\,nm}$ 160 $M^{-1}\,cm^{-1}$ (ref 11)

[a] ϵ = molar absorbance.

contribute to the absorbance change in the studied wavelength region.

Discussion

The results obtained here provide further evidence for the formation of transient bi- and tetranuclear complexes between the iron(III) hydroxo dimer and simple inorganic ligands. With the exception of the arsenite system, the absorbance decay at the characteristic band of $Fe_2(OH)_2^{4+}$ could be used to obtain quantitative information for the equilibrium and kinetic features of these complexes. However, the catalytic effect of arsenite ion on the monomer−dimer hydrolytic equilibrium of iron(III) also indicates the formation of such a complex at very low concentration levels.

In the sulfate ion system, the data are consistent with the immeasurably fast formation of a relatively weak binuclear complex. It should be noted that eq 18 reflects only the overall stoichiometry for the reaction which may proceed via either HSO_4^- and/or SO_4^{2-}. These two forms are always present in comparable concentrations, and it is very likely that the SO_4^{2-} path is predominant as deprotonation of a ligand typically enhances its reactivity.

The rest of the reactions show very similar kinetic patterns. After fast accumulation of the multinuclear species, it is gradually transformed into the corresponding mono complex. In some systems, the formation of Fe_nL is well separated from other reaction steps and can be studied independently under pseudo-first-order conditions. In other cases, the formation and subsequent decay of the multinuclear complex are kinetically coupled, and comprehensive data treatment is required.

The rate constants for the complex formation of the hydroxo dimer with different protonated forms of various ligands are compared in Table 5. Significant differences were not found between the rate constants of the neutral as well as the uninegatively charged forms of the different ligands implying that specific interactions are not operative in these reactions. The results strongly suggest that these reactions proceed via a dissociative interchange, I_d, mechanism, and the proton-transfer steps associated with the loss of a ligand proton and an OH bridge do not affect the overall rate. Thus, $k = k_{ex}K_{ip}$ applies, where k, k_{ex}, and K_{ip} are the rate constant of the complex formation, the rate constant of the water exchange between the hydroxo dimer and the bulk water, and the ion pair stability constant between the reactants, respectively. The 10−30 times difference between the rate constants of the two forms of the same ligand supports these considerations. This trend can conveniently be explained in terms of the charge products of the reactants, as the Fuoss equation predicts an about 15 times difference in the stability of the corresponding outer sphere complexes.[43] It follows that the water exchange rate constant of the dimer must be on the order of $10^5\ s^{-1}$. For comparison, the water exchange rate constants of $Fe(H_2O)_6^{3+}$ and $Fe(H_2O)_5OH^{2+}$ are $1.6 \times 10^2\ s^{-1}$ and $1.2 \times 10^5\ s^{-1}$, respectively.[44] It is reasonable to assume that the source of the relatively high lability is the same in both the mononuclear and dimer hydroxo complexes which is the labilizing effect of the hydroxide group.

The previous interpretation does not apply to the dinegative SO_3^{2-} ion. In this case, $K_{ip} = 24\ M^{-1}$ would be consistent with a difference of about 1 order of magnitude between the rate constants of HSO_3^- and SO_3^{2-}. The reason for the very high, almost diffusion controlled second-order rate constant of the SO_3^{2-} pathway is not apparent; it may be related to specific features of aqueous sulfur(IV).

Thorough structural characterization of the multinuclear intermediates seems to be beyond experimental limitations because the lifetimes of these species do not exceed a few seconds in solution. For the same reason, preparation of the corresponding solid salts of the complexes is not feasible. Therefore, any conclusion regarding the structures of these species is based on plausible chemical considerations and comparison of the available kinetic and thermodynamic data.

Earlier, we proposed that only those ligands are suitable to form multinuclear complexes with the hydroxo dimer which are capable of replacing a hydroxo bridge between the two iron(III) centers.[16] The results presented here seem to corroborate this assumption because such complexes were found only with oxoanions. It can be inferred that the appropriate geometry of the ligand, most significantly the O−X−O angle, is a key factor in these reactions. Most likely, this is the reason why several ligands, such as halogenate ions, acetate ion and its derivatives, and so forth, do not react directly with the hydroxo dimer although they also contain the O−X−O motif.

In the studied systems, the formation of the Fe_nL complex is sort of a dead-end reaction as the thermodynamically stable product is always the corresponding mononuclear complex

(43) Fuoss, R. M. *J. Am. Chem. Soc.* **1958**, *80*, 5059.
(44) Grant, M.; Jordan, R. B. *Inorg. Chem.* **1981**, *20*, 55.

of iron(III). The rates of the fast formation and the considerably slower dissociation of the multinuclear complex into Fe_{mon} and FeL show the same pH dependencies in each case. This is a strong indication that the two reactions proceed via the same intermediate in which the ligand is presumably coordinated to only one Fe(III) center. As expected, the replacement of one OH bridge by the ligand and the formation of the Fe_2L complex is kinetically more favorable than asymmetric dissociation of the intermediate into mononuclear species. This trend is clearly demonstrated by the differences of the corresponding rate constants.

In conclusion, direct ligand substitution reactions with the hydroxo dimer can be a general feature in aqueous chemistry of iron(III). Such reactions may also occur under conditions considerably different from the ones used in the present study. In this respect, it is worth noting that, while the solubility of iron(III) decreases, the mole fractions of the dimer and multinuclear hydroxo species increase by increasing the pH. Therefore, when less acidic conditions are used, fast formation of multinuclear iron(III) complexes may prove to be important for the interpretation of the kinetic data even at low iron(III) concentrations and ligand excess. Proper description of such reactions seems to be crucial in order to explore the exact role of iron(III) in composite reactions of environmental and biochemical significance.

Acknowledgment. This work was supported by the Hungarian National Research Foundation under Grants OTKA M 028244 and T 029568.

Supporting Information Available: Extended graphs and tables (15 pages). This material is available free of charge via Internet at htttp://pubs.acs.org.

IC011013W